

Article

Exact Traveling and Nano-Solitons Wave Solitons of the Ionic Waves Propagating along Microtubules in Living Cells

Abdel-Haleem Abdel-Aty ^{1,2} , Mostafa M. A. Khater ^{3,4,*} , Raghda A. M. Attia ^{3,5} and Hichem Eleuch ^{6,7} 

¹ Department of Physics, College of Sciences, University of Bisha, P.O. Box 344, Bisha 61922, Saudi Arabia; amabdelaty@ub.edu.sa

² Physics Department, Faculty of Science, Al-Azhar University, 71524 Assiut, Egypt

³ Department of Mathematics, Faculty of Science, Jiangsu University, Jiangsu 212013, China; Raghda.attia2024@yahoo.com

⁴ Department of Mathematics, El Obour Institutes, 11828 Cairo, Egypt

⁵ Department of Basic Science, Higher Technological Institute, 44634 10th of Ramadan City, Egypt

⁶ Department of Applied Science and Mathematics, College of Arts and Sciences, Abu Dhabi University, Abu Dhabi 59911, UAE; hichemeleuch@yahoo.fr

⁷ Institute for Quantum Science and Engineering, Texas A&M University, College Station, TX 77843, USA

* Correspondence: mostafa.khater2024@yahoo.com

Received: 24 March 2020; Accepted: 20 April 2020; Published: 2 May 2020



Abstract: In this paper, the weakly nonlinear shallow-water wave model is mathematically investigated by applying the modified Riccati-expansion method and Adomian decomposition method. This model is used to describe the propagation of waves in weakly nonlinear and dispersive media. We obtain exact and solitary wave solutions of this model by using the modified Riccati-expansion method then using these solutions to determine the boundary and initial conditions. These conditions are employed to evaluate the semi-analytical wave solutions and calculate the absolute value of error. The values of absolute error show the accuracy of the obtained solutions. Some solutions are sketched to show the perspective view of the solution of this model. Moreover, the novelty of the obtained solutions is illustrated by showing the similarity and differences between our and previous solutions of the model.

Keywords: the modified Riccati expansion method; Adomian decomposition method (ADM); weakly nonlinear shallow-water wave regime; analytical and semi-analytical wave solutions

1. Introduction

Nonlinearity has recently been considered as the generator of many complex phenomena in distinct fields such as infectious disease epidemiology [1], neural networks [2], biology [3], fluid mechanics [4], population ecology [5], solid-state physics [6], wave propagation in plasma physics [7], thermodynamics [8], condensed matter physics [9], nonlinear optics [10], civil engineering [11], quantum mechanics [12], plasma wave [13], soil mechanics [14], and so on; they are formulated in nonlinear evolution equations. The mathematical formulation of this phenomenon depends on real experiments to determine the parameters and empirical functions. These obtained mathematical formulas help us to understand these complex phenomena by explaining their physical and dynamical behavior. Thus, many mathematical and physical researchers have paid attention to solve these nonlinear evolution equations. These works have been deriving many analytical and numerical mathematical schemes to construct analytical, semi-analytical, approximate solutions. These schemes are based on three mainly channels, namely Lie group techniques, reduction techniques and ansatz techniques [15–29].

The main goal of this article is to study one of the nonlinear evolution equations (the ionic waves propagating along microtubules in living cells) that is used to study the propagation of waves in weakly nonlinear and dispersive media. Our study applies two computational schemes [30–39] to this model for constructing exact traveling and solitary wave solutions. Moreover, we calculate the values of absolute error to show the power and accuracy of our obtained solutions.

Firstly, the direction of flow for a fluid with a constant depth of μ with the following properties—non-rotating flow, incompressible, and inviscid, x -axis and z -axis positively upward the free surface in the gravitational field. The free surface elevation is above the undisturbed depth μ is $\zeta(x, t)$, so that the wave surface at height $z = \mu + \zeta(x, t)$, while $z = 0$ is a horizontal rigid bottom. Moreover, the Laplace and Euler equation with the boundary conditions at the surface and at the bottom, respectively, are given by

$$\left\{ \begin{array}{ll} \mathcal{A}_{xx} + \mathcal{A}_{zz} = 0, & 0 < z < \mu + \zeta \\ \mathcal{A}_t + \frac{1}{2} (\mathcal{A}_x \vec{i} + \mathcal{A}_z \vec{k})^2 + \lambda \zeta = 0 & z = \mu + \zeta \\ \zeta_t + \zeta_x \mathcal{A}_x - \mathcal{A}_z = 0, & \\ \mathcal{A}_z = 0, & z = 0. \end{array} \right. \tag{1}$$

This is considered a good start to define the next dimensionless parameters:

$$\omega = \frac{\zeta_0}{\mu} < 1; \quad \Xi = \left(\frac{\mu}{\zeta}\right)^2 < 1, \tag{2}$$

where ζ_0 is the wave amplitude, and ζ is the characteristic length-like wavelength. Accordingly, we also take a complete set of new suitable non-dimensional variables:

$$X = \frac{x}{\zeta}; \quad Z = \frac{z}{\mu}; \quad \tau = \frac{ct}{\zeta} \quad \Psi = \frac{\zeta}{\zeta_0} \quad \Phi = \frac{\mu}{\zeta_0 \zeta c} \mathcal{A}, \tag{3}$$

where $c = \sqrt{g\mu}$ is the shallow-water wave speed, with g being gravitational acceleration so that we get:

$$\left\{ \begin{array}{ll} \Xi \mathcal{A}_{XX} + \mathcal{A}_{ZZ} = 0, & \\ \Phi_\tau + \frac{\omega}{2\Xi} (\Phi_X)^2 + \frac{\omega}{2\Xi} (\Phi_Z) + \Psi = 0, & Z = 1 + \omega \Psi, \\ \Psi_\tau + \omega (\Phi_X \Psi_X) - \frac{1}{\Xi} \Phi_Z = 0, & Z = 1 + \omega \Psi, \\ \Phi_Z = 0, & Z = 0 \end{array} \right. \tag{4}$$

Expanding $\Phi(x, \tau)$ in terms of Ξ , yields

$$\Phi = \Phi_0 + \Xi \Phi_1 + \Xi^2 \Phi_2, \tag{5}$$

using the dimensionless wave particles velocity in x -direction, by the definition $v = \Phi_X$, leads to

$$\left\{ \begin{array}{l} (\Phi_0)_\tau - \frac{\Xi}{2} v_{\tau X} + \Psi + \frac{1}{2} \omega v^2 = 0, \\ \Psi_\tau + \omega v \Psi_X + \frac{1}{\Xi} (1 + \omega \Psi) v_X = \frac{\Xi}{6} v_{XX}. \end{array} \right. \tag{6}$$

Making the differentiation of the first equation of Equation (6) with respect to X , and rearranging the second equation of the same system, leads to

$$\left\{ \begin{array}{l} v_\tau + \omega v v_X + \Psi_X - \frac{\Xi}{2} v_{X\tau} = 0, \\ \Psi_\tau + (v(1 + \omega \Psi))_X - \frac{\Xi}{6} v_{XX} = 0. \end{array} \right. \tag{7}$$

Returning back to dimensional variables $\zeta(x, t)$ and $\mathcal{E} = \Phi_x$, yields

$$\mathcal{E}_t + \mathcal{E} \mathcal{E}_x + \lambda \zeta_x = \frac{1}{3} \mu^2 \mathcal{E}_{xxt}. \tag{8}$$

We could define the new function $\mathcal{E}(x, t)$ unifying the velocity and displacement of water particles as follows:

$$\mathcal{E} = \frac{1}{\mu} \mathcal{H}_t, \quad \zeta = -\mathcal{H}_x. \tag{9}$$

So that the weakly nonlinear shallow water wave equation is given by [40–44]

$$\mathcal{H}_{tt} - \lambda \mu \mathcal{H}_{xx} + \frac{1}{2\mu} (\mathcal{H}_t^2)_x - \frac{\mu^2}{3} \mathcal{H}_{xxtt} = 0, \quad x, t \in \mathcal{R}, \tag{10}$$

where $\mathcal{R} =] - \infty, \infty[$, $\mathcal{H} = \mathcal{H}(x, t)$ unifying the velocity and displacement of water particles, μ is the wave height and λ is the gravitation force. Using the moving coordinate $[\mathcal{H} = \mathcal{H}(x, t) = \mathcal{U}(Y), Y = x - \mathcal{U}t]$ with wave speed (\mathcal{U}) converts Equation (10) into the following ordinary nonlinear differential equation:

$$(\mathcal{U}^2 - \lambda \mu) \mathcal{U}'' + \frac{\mathcal{U}^2}{2\mu} (\mathcal{U}^2)' - \frac{\mathcal{U}^2 \mu^2}{3} \mathcal{U}'''' = 0. \tag{11}$$

Integration Equation (11) once with zero constant of the integration, and replacing $\mathcal{U}(Y)$ with $[\int \mathcal{S}(Y) dY]$, leads to

$$\mathcal{S}'' - (a \mathcal{S}^2 + b \mathcal{S} + c) = 0, \tag{12}$$

where $[a = \frac{3}{2\mu^3}, b = \frac{3(\mathcal{U}^2 - \lambda \mu)}{(\mathcal{U} \mu)^2}]$, while c is the integration constant. The replacement between $\mathcal{U}(Y)$ and $\mathcal{S}(Y)$ aims to simplify Equation (11) into its simplest form. Applying the following homogeneous balance rule

$$D \left[\frac{d^q \mathcal{S}}{d\xi^q} \right] = m + q, \quad D \left[\mathcal{S}^p \left(\frac{d^q \mathcal{S}}{d\xi^q} \right)^s \right] = mp + s(m + q), \tag{13}$$

to Equation (12) yields, $(\mathcal{S}'' \ \& \ \mathcal{S}^2) \Rightarrow (2m = m + 2) \Rightarrow (m = 2)$.

The rest of the paper is organized as follows. Section 2 employs two analytical and semi-analytical schemes to find distinct types of solutions for the model. The goals of this section are constructing the exact traveling and solitary wave solutions of the suggested model then evaluating the initial and boundary conditions that allows application of the Adomian decomposition method for finding the semi-analytical wave solutions. Finally, we estimate the absolute value of error to show the accuracy of the obtained solutions. Section 3 shows the physical and dynamical behaviour of our obtained solutions. Moreover, the novelty of our results is explained by comparing our solutions with previous obtained solutions. Section 4 gives the conclusion.

2. Application

This section handles the analytical and semi-analytical wave solutions of the weakly nonlinear shallow water wave model by employing two recent computational schemes.

2.1. Explicit Analytical Wave Solutions

Applying the modified Riccati-expansion method to Equation (12), yields formulating its general wave solutions in the following formula:

$$\mathcal{S} = \sum_{i=1}^m a_i \Lambda(Y)^i + a_0 = a_2 \Lambda(Y)^2 + a_1 \Lambda(Y) + a_0, \tag{14}$$

where $[a_0, a_1, a_2]$ are arbitrary constants to be determined later. Additionally, $\Lambda(Y)$ is the solution function of the following ordinary differential equation

$$\Lambda'(Y) = \delta\Lambda(Y) + \sigma\Lambda(Y)^2 + \varrho, \tag{15}$$

where $[\delta, \sigma, \varrho]$ are arbitrary constants. Substituting Equation (14) along (15) into Equation (12), and collecting all terms with the same power of $[\Lambda(Y)^i, i = 0, 1, 2, 3, 4]$, yield a system of algebraic equations. Using a computer software program (Mathematica 12) to solve this system, leads to

$$\left[a_0 \rightarrow \frac{-b + \delta^2 + 8\sigma\varrho}{2a}, a_1 \rightarrow \frac{6\delta\sigma}{a}, a_2 \rightarrow \frac{6\sigma^2}{a}, c \rightarrow \frac{b^2 - \delta^4 + 8\delta^2\sigma\varrho - 16\sigma^2\varrho^2}{4a}, \text{ where } (a \neq 0) \right].$$

Thus, the computational wave solutions of Equation (12) have the following formulas:

For $[\delta^2 - 4\sigma\varrho > 0 \ \& \ \delta\sigma \neq 0]$

$$\mathcal{S}_1(x, t) = \frac{-1}{2a} \left[b - \delta^2 + 3(\delta^2 - 4\sigma\varrho) \operatorname{sech}^2 \left(\frac{1}{2} \sqrt{\delta^2 - 4\sigma\varrho} (tU + x) \right) + 4\sigma\varrho \right], \tag{16}$$

$$\mathcal{S}_2(x, t) = \frac{1}{2a} \left[-b + \delta^2 + 3(\delta^2 - 4\sigma\varrho) \operatorname{csch}^2 \left(\frac{1}{2} \sqrt{\delta^2 - 4\sigma\varrho} (tU + x) \right) - 4\sigma\varrho \right]. \tag{17}$$

For $[\delta^2 - 4\sigma\varrho < 0 \ \& \ \delta\sigma \neq 0]$

$$\mathcal{S}_3(x, t) = \frac{-1}{2a} \left[b + 2\delta^2 + 3(\delta^2 - 4\sigma\varrho) \tan^2 \left(\frac{1}{2} \sqrt{4\sigma\varrho - \delta^2} (tU + x) \right) - 8\sigma\varrho \right], \tag{18}$$

$$\mathcal{S}_4(x, t) = \frac{-1}{2a} \left[b + 2\delta^2 + 3(\delta^2 - 4\sigma\varrho) \cot^2 \left(\frac{1}{2} \sqrt{4\sigma\varrho - \delta^2} (tU + x) \right) - 8\sigma\varrho \right]. \tag{19}$$

For $[\delta^2 - 4\sigma\varrho > 0 \ \& \ \sigma\varrho \neq 0]$

$$\mathcal{S}_5(x, t) = \frac{1}{2a} \left[-b + \delta^2 + \frac{24\sigma^2\varrho^2 (\cosh(\sqrt{\delta^2 - 4\sigma\varrho} (tU + x)) + 1)}{(\delta \cosh(\frac{1}{2} \sqrt{\delta^2 - 4\sigma\varrho} (tU + x)) - \sqrt{\delta^2 - 4\sigma\varrho} \sinh(\frac{1}{2} \sqrt{\delta^2 - 4\sigma\varrho} (tU + x)))^2} - \frac{24\delta\sigma\varrho}{\delta - \sqrt{\delta^2 - 4\sigma\varrho} \tanh(\frac{1}{2} \sqrt{\delta^2 - 4\sigma\varrho} (tU + x))} + 8\sigma\varrho \right], \tag{20}$$

$$\mathcal{S}_6(x, t) = \frac{1}{2a} \left[-b + \delta^2 + \frac{24\sigma^2\varrho^2 (\cosh(\sqrt{\delta^2 - 4\sigma\varrho} (tU + x)) - 1)}{(\sqrt{\delta^2 - 4\sigma\varrho} \cosh(\frac{1}{2} \sqrt{\delta^2 - 4\sigma\varrho} (tU + x)) - \delta \sinh(\frac{1}{2} \sqrt{\delta^2 - 4\sigma\varrho} (tU + x)))^2} - \frac{24\delta\sigma\varrho}{\delta - \sqrt{\delta^2 - 4\sigma\varrho} \coth(\frac{1}{2} \sqrt{\delta^2 - 4\sigma\varrho} (tU + x))} + 8\sigma\varrho \right]. \tag{21}$$

For $[\delta^2 - 4\sigma\varrho < 0 \ \& \ \sigma\varrho \neq 0]$

$$S_7(x, t) = \frac{1}{2a} \left[-b + \delta^2 + \frac{24\sigma^2\varrho^2 \left(\cos(\sqrt{4\sigma\varrho - \delta^2}(tU+x)) + 1 \right)}{\left(\sqrt{4\sigma\varrho - \delta^2} \sin\left(\frac{1}{2}\sqrt{4\sigma\varrho - \delta^2}(tU+x)\right) + \delta \cosh\left(\frac{1}{2}\sqrt{4\sigma\varrho - \delta^2}(tU+x)\right) \right)^2} - \frac{24\delta\sigma\varrho \cos\left(\frac{1}{2}\sqrt{4\sigma\varrho - \delta^2}(tU+x)\right)}{\sqrt{4\sigma\varrho - \delta^2} \sin\left(\frac{1}{2}\sqrt{4\sigma\varrho - \delta^2}(tU+x)\right) + \delta \cosh\left(\frac{1}{2}\sqrt{4\sigma\varrho - \delta^2}(tU+x)\right)} + 8\sigma\varrho \right], \tag{22}$$

$$S_8(x, t) = \frac{1}{2a} \left[-b + \delta^2 - \frac{24\sigma^2\varrho^2 \left(\cos(\sqrt{4\sigma\varrho - \delta^2}(tU+x)) - 1 \right)}{\left(\sqrt{4\sigma\varrho - \delta^2} \cos\left(\frac{1}{2}\sqrt{4\sigma\varrho - \delta^2}(tU+x)\right) - \delta \sinh\left(\frac{1}{2}\sqrt{4\sigma\varrho - \delta^2}(tU+x)\right) \right)^2} + \frac{24\delta\sigma\varrho \sin\left(\frac{1}{2}\sqrt{4\sigma\varrho - \delta^2}(tU+x)\right)}{\sqrt{4\sigma\varrho - \delta^2} \cos\left(\frac{1}{2}\sqrt{4\sigma\varrho - \delta^2}(tU+x)\right) - \delta \sinh\left(\frac{1}{2}\sqrt{4\sigma\varrho - \delta^2}(tU+x)\right)} + 8\sigma\varrho \right]. \tag{23}$$

For $\left[\varrho = 0 \ \& \ \delta\sigma \neq 0 \right]$

$$S_9(x, t) = \frac{1}{2a} \left[\delta^2 \left(\frac{12\sigma\Omega e^{\delta(tU+x)} \left(\Omega(\sigma - \beta)e^{\delta(tU+x)} - \beta \right)}{\left(\beta + \beta\Omega e^{\delta(tU+x)} \right)^2} + 1 \right) - b \right], \tag{24}$$

$$S_{10}(x, t) = \frac{1}{2a} \left[\delta^2 \left(1 - \frac{12\sigma e^{\delta(tU+x)} \left(\beta\Omega + (\beta - \sigma)e^{\delta(tU+x)} \right)}{\beta^2 \left(e^{\delta(tU+x)} + \Omega \right)^2} \right) - b \right]. \tag{25}$$

where $\left[\Omega, \beta \right]$ are arbitrary constants.

2.2. Semi-Analytical Wave Solutions

Applying the Adomian decomposition method to Equation (12) with the solution Equation (16) under the following conditions

$$\left[a = 5, b = 4, c = \frac{3}{4}, \delta = 3, \sigma = 2, \varrho = 1, S = \frac{1}{10} \left(-3\operatorname{sech}^2\left(\frac{Y}{2}\right) - 3 \right) \right],$$

yield, the following semi-analytical solutions of Equation (18)

$$S_0 = \frac{3Y^2}{8} - \frac{3}{5}, \tag{26}$$

$$S_1 = \frac{3Y^6}{128} - \frac{Y^4}{16} - \frac{3Y^2}{10}, \tag{27}$$

$$S_2 = \frac{Y^{10}}{1024} - \frac{9Y^8}{1792} - \frac{Y^6}{30} + \frac{Y^4}{20}, \tag{28}$$

$$S_3 = \frac{45Y^{14}}{2981888} - \frac{Y^{12}}{12288} + \frac{61Y^{10}}{322560} - \frac{11Y^8}{1920} - \frac{Y^6}{300} + \frac{3Y^4}{20}. \tag{29}$$

Thus, the approximate solution of Equation (18) is calculated in the following form:

$$S_{\text{approximate}} = \frac{45Y^{14}}{2981888} - \frac{Y^{12}}{12288} + \frac{47Y^{10}}{40320} - \frac{289Y^8}{26880} - \frac{127Y^6}{9600} + \frac{11Y^4}{80} + \frac{3Y^2}{40} - \frac{3}{5}. \tag{30}$$

Now, we evaluate the obtained analytical and semi-analytical solutions for different values of Y to show the absolute values of error between them. Table 1 shows the accuracy of solutions where the absolute value of error is very small.

Table 1. Values of computational and semi-analytical solutions for different values of Y to show the accuracy of the obtained solutions.

Value of Y	Analytical Solution	Semi-Analytical Solutions	Absolute Value of Error
0.01	0.599993	0.599992	1.49999×10^{-9}
0.02	0.59997	0.59997	2.3999×10^{-8}
0.03	0.599933	0.599932	1.21489×10^{-7}
0.04	0.59988	0.59988	3.83938×10^{-7}
0.05	0.599813	0.599812	9.37265×10^{-7}
0.06	0.59973	0.599728	1.9433×10^{-6}
0.07	0.599633	0.599629	3.59973×10^{-6}
0.08	0.599521	0.599514	6.14005×10^{-6}
0.09	0.599393	0.599383	9.83348×10^{-6}
0.1	0.599251	0.599236	1.49849×10^{-5}

3. Results and Discussion

Here, we discuss our obtained analytical and semi-analytical solutions of the weakly nonlinear shallow-water wave model.

1. The modified Riccati expansion method and Adomian decomposition method were applied to the weakly nonlinear shallow water wave equation for constructing the exact traveling and semi-analytical wave solutions. These methods are considered as recent schemes in this field and they were not applied to this model previously.
2. All our obtained solutions are different from that obtained in References [40,44] where the authors of References [40,44] applied different methods to solve the weakly nonlinear shallow water wave regime.
3. Equations (29) and (30) equal to Equations (8) and (9) [45], when $\left[a = \frac{-1}{2}, b + 2\delta^2 - 8\sigma\varrho = \frac{8b-\beta}{2\alpha}, \frac{6b}{\alpha} = 3(\delta^2 - 4\sigma\varrho), 4b = (4\sigma\varrho - \delta^2) \right]$ while all our obtained solutions are different from that obtained in this paper where the Khater method was employed to find the exact traveling and solitary wave solutions.
4. Figure 1 shows the breath wave solution Equation (16) in the three-dimensional plot (a) to illustrate the perspective view of the solution, the two-dimensional plot (b) to present the wave propagation pattern of the wave along x-axis, and the contour plot (c) to explain the overhead view of the solution when $\left[a = 5, b = 4, \delta = 3, \sigma = 2, \varrho = 1, U = -1 \right]$.
5. Figure 2 shows the kink wave solution Equation (20) in the three-dimensional plot (a) to clarify the perspective view of the solution, the two-dimensional plot (b) to illustrate the wave propagation pattern of the wave along x-axis, and the contour plot (c) to exhibit the overhead view of the solution when $\left[a = 2, b = 4, \delta = 5, \sigma = 6, \varrho = 1, U = 3 \right]$.
6. Figure 3 shows the periodic-wave solution Equation (24) in the three-dimensional plot (a) to exalt the perspective view of the solution, the two-dimensional plot (b) to exhibit the wave propagation pattern of the wave along x-axis, and the contour plot (c) to explain the overhead view of the solution when $\left[a = 2, b = 4, \beta = -6, \delta = 5, \sigma = 6, \Omega = -5, \varrho = 0, U = 3 \right]$.
7. Figure 4 shows the cone-wave solution Equation (30) in the three-dimensional plot (a) to illustrate the perspective view of the solution, the two-dimensional plot (b) to explain the wave propagation pattern of the wave along x-axis, and the contour plot (c) to clarify the overhead view of the solution when $\left[U = -3 \right]$.
8. Figure 5 shows the distinct types of plots of Table 1 in line plot (a), columns plot (b), and scattering plot (c). These figures show the accuracy of the obtained analytical wave solutions compared to the approximate solutions.

9. Table 1 shows the accuracy of the obtained analytical where the absolute value of error between analytical and semi-analytical solutions are imperceptible.

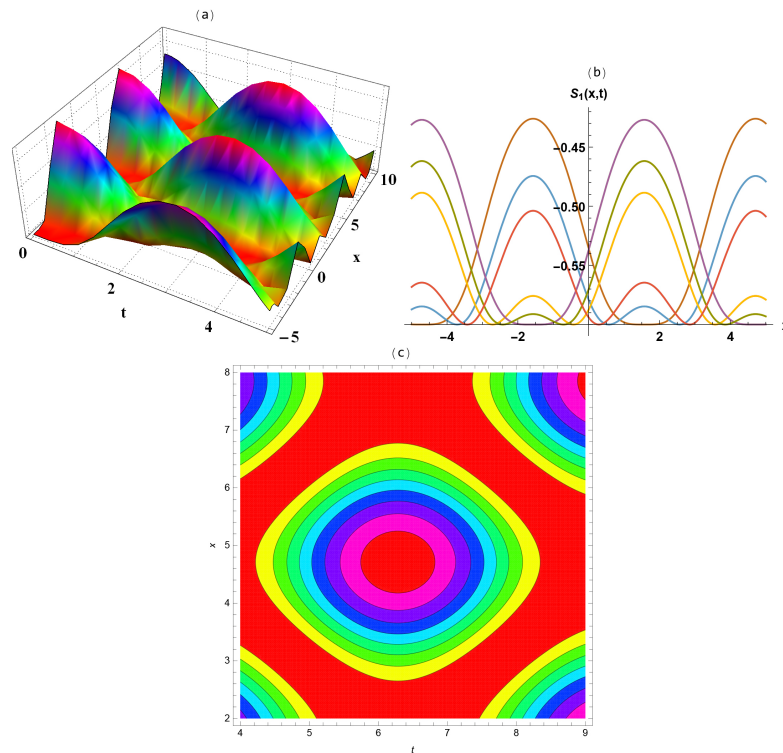


Figure 1. Numerical simulation of Equation (16) in three (a), two-dimensional (b), and contour (c) sketches for $[a = 5, b = 4, \delta = 3, \sigma = 2, \rho = 1, \mathcal{U} = -1]$.

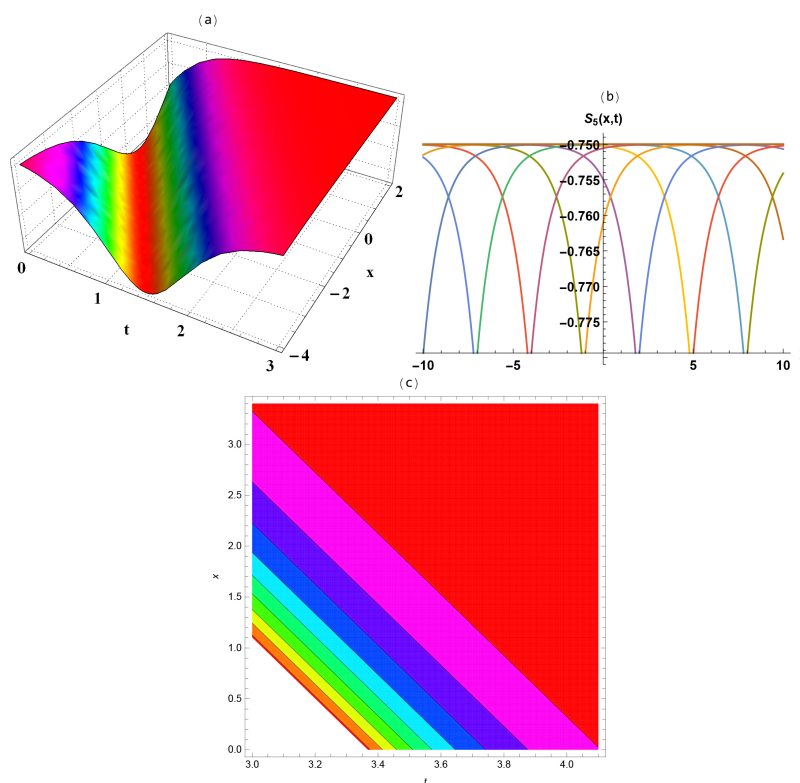


Figure 2. Numerical simulation of Equation (20) in three (a), two-dimensional (b), and contour (c) sketches for $[a = 2, b = 4, \delta = 5, \sigma = 6, \rho = 1, \mathcal{U} = 3]$.

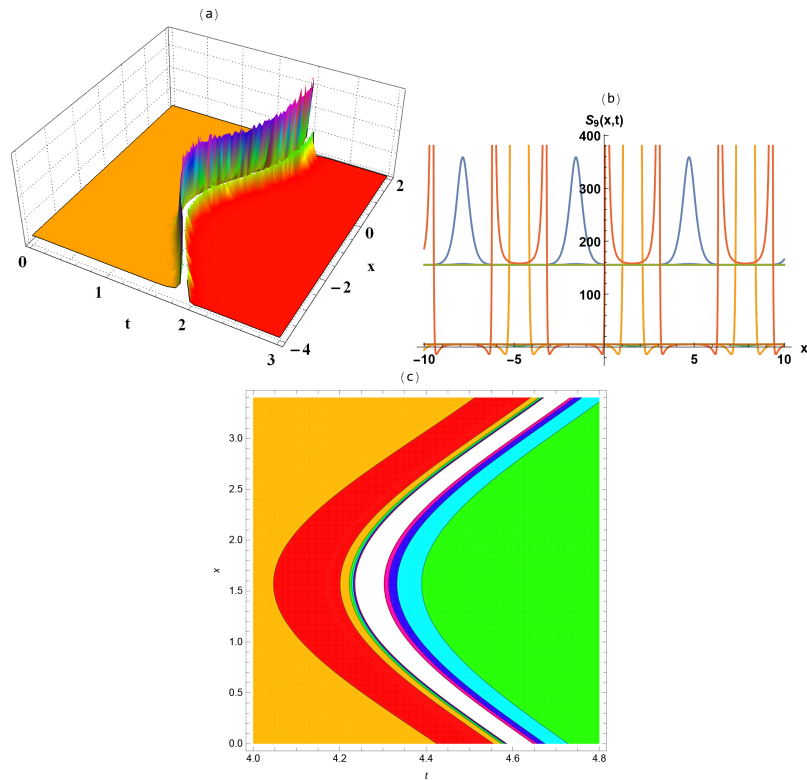


Figure 3. Numerical simulation of Equation (24) in three (a), two-dimensional (b), and contour sketches (c) for $[a = 2, b = 4, \beta = -6, \delta = 5, \sigma = 6, \Omega = -5, \varrho = 0, \bar{U} = 3]$.

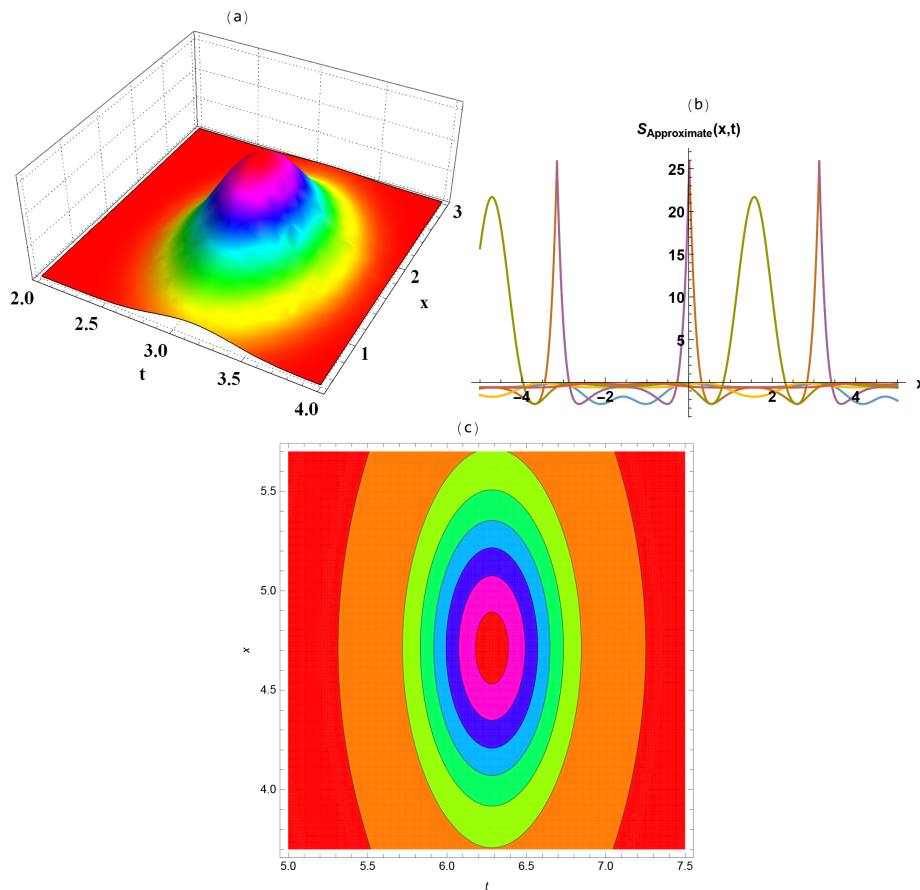


Figure 4. Numerical simulation of Equation (30) in three (a), two-dimensional (b), and contour sketches (c).

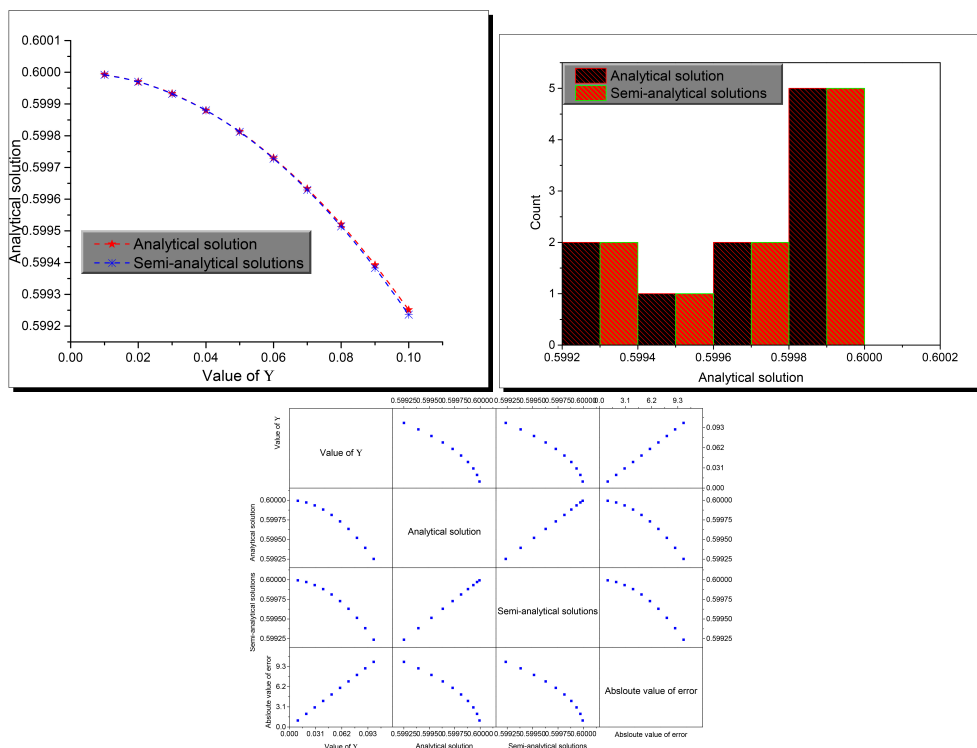


Figure 5. Sketches of Computational and semi-analytical solutions in distinct plots to show the accuracy of the obtained solutions.

4. Conclusions

New distinct types of the ocean solitons to cellular ionic nano-solitons of the nonlinear weakly nonlinear shallow-water wave regime have been investigated by using two recent analytical and semi-analytical schemes. Some new soliton wave solutions were obtained plotted in two, three-dimensional, and contour plots of these solutions. The effectiveness and power of the used methods and their ability for application to other nonlinear evaluation equation are illustrated.

Author Contributions: Investigation, M.M.A.K.; methodology, M.M.A.K.; software, R.A.M.A.; supervision, A.-H.A.-A. and H.E.; writing—review & editing, H.E. All authors have read and agreed to the published version of the manuscript.

Funding: This research received no external funding.

Conflicts of Interest: The authors declare no conflict of interest.

References

1. Brinks, R.; Hoyer, A. Illness-death model: Statistical perspective and differential equations. *Lifetime Data Anal.* **2018**, *24*, 743–754. [[CrossRef](#)] [[PubMed](#)]
2. Mellit, A.; Eleuch, H.; Benghanem, M.; Elaoun, C.; Pavan, A.M. An adaptive model for predicting of global, direct and diffuse hourly solar irradiance. *Energy Convers. Manag.* **2010**, *51*, 771–782. [[CrossRef](#)]
3. Barfield, M.; Martcheva, M.; Tuncer, N.; Holt, R.D. Backward bifurcation and oscillations in a nested immuno-eco-epidemiological model. *J. Biol. Dyn.* **2018**, *12*, 51–88. [[CrossRef](#)]
4. Xu, Z.; Chow, K. Breathers and rogue waves for a third order nonlocal partial differential equation by a bilinear transformation. *Appl. Math. Lett.* **2016**, *56*, 72–77. [[CrossRef](#)]
5. Lin, Y.; Gao, J. Research on Diffusion Effect of Ecological Population Model Based on Delay Differential Equation. *Caribb. J. Sci.* **2019**, *52*, 333–335.
6. He, Z.; Han, Z.; Yuan, J.; Sinyukov, A.M.; Eleuch, H.; Niu, C.; Zhang, Z.; Lou, J.; Hu, J.; Voronine, D.V.; et al. Quantum plasmonic control of trions in a picocavity with monolayer WS₂. *Sci. Adv.* **2019**, *5*, eaau8763. [[CrossRef](#)]

7. Cheemaa, N.; Seadawy, A.R.; Chen, S. Some new families of solitary wave solutions of the generalized Schamel equation and their applications in plasma physics. *Eur. Phys. J. Plus* **2019**, *134*, 117. [[CrossRef](#)]
8. Granados, S.; Salazar, M.; Toral, R.; Tavera, R.; Velázquez, A.; Hernández, L.; Cid, R.; López, G.; González, R. Pressure wave equation far from thermodynamics equilibrium. *J. Phys. Conf. Ser.* **2019**, *1221*, 012055. [[CrossRef](#)]
9. Odashima, M.M.; Prado, B.G.; Vernek, E. Pedagogical introduction to equilibrium Green's functions: Condensed-matter examples with numerical implementations. *Revista Brasileira de Ensino de Física* **2017**, *39*. [[CrossRef](#)]
10. Newell, A. *Nonlinear Optics*; CRC Press: Boca Raton, FL, USA, 2018.
11. Baudouin, L.; Rondepierre, A.; Neild, S. Robust control of a cable from a hyperbolic partial differential equation model. *IEEE Trans. Control Syst. Technol.* **2018**, *27*, 1343–1351. [[CrossRef](#)]
12. Laskin, N. Nonlocal quantum mechanics: Fractional calculus approach. *Appl. Phys.* **2019**, 207–236. [[CrossRef](#)]
13. Vallejos, P.; Johnson, T.; Hellsten, T. Modeling RF waves in spatially dispersive inhomogeneous plasma using an iterative wavelet spectral method. In *EPJ Web of Conferences*; EDP Sciences: Les Ulis, France, 2017; Volume 157, p. 03059.
14. Shao, L.; Guo, X.; Liu, S.; Zheng, G. *Effective Stress and Equilibrium Equation for Soil Mechanics*; CRC Press: Boca Raton, FL, USA, 2017.
15. Rezazadeh, H.; Kumar, D.; Neirameh, A.; Eslami, M.; Mirzazadeh, M. Applications of three methods for obtaining optical soliton solutions for the Lakshmanan–Porsezian–Daniel model with Kerr law nonlinearity. *Pramana* **2020**, *94*, 39. [[CrossRef](#)]
16. Mirhosseini-Alizamini, S.M.; Rezazadeh, H.; Eslami, M.; Mirzazadeh, M.; Korkmaz, A. New extended direct algebraic method for the Tzitzica type evolution equations arising in nonlinear optics. *Comput. Methods Differ. Equ.* **2020**, *8*, 28–53.
17. Souleymanou, A.; Korkmaz, A.; Rezazadeh, H.; Mukam, S.P.T.; Bekir, A. Soliton solutions in different classes for the Kaup–Newell model equation. *Mod. Phys. Lett. B* **2020**, *34*, 2050038. [[CrossRef](#)]
18. Attia, R.A.; Lu, D.; Ak, T.; Khater, M.M. Optical wave solutions of the higher-order nonlinear Schrödinger equation with the non-Kerr nonlinear term via modified Khater method. *Mod. Phys. Lett. B* **2020**, *34*, 2050044. [[CrossRef](#)]
19. Khater, M.M.; Park, C.; Abdel-Aty, A.H.; Attia, R.A.; Lu, D. On new computational and numerical solutions of the modified Zakharov–Kuznetsov equation arising in electrical engineering. *Alex. Eng. J.* **2020**. [[CrossRef](#)]
20. Khater, M.M.; Attia, R.A.; Abdel-Aty, A.H.; Abdou, M.; Eleuch, H.; Lu, D. Analytical and semi-analytical ample solutions of the higher-order nonlinear Schrödinger equation with the non-Kerr nonlinear term. *Results Phys.* **2020**, *16*, 103000. [[CrossRef](#)]
21. Park, C.; Khater, M.M.; Attia, R.A.; Alharbi, W.; Alodhaibi, S.S. An explicit plethora of solution for the fractional nonlinear model of the low-pass electrical transmission lines via Atangana–Baleanu derivative operator. *Alex. Eng. J.* **2020**. [[CrossRef](#)]
22. Khater, M.M.; Attia, R.A.; Baleanu, D. Abundant new solutions of the transmission of nerve impulses of an excitable system. *Eur. Phys. J. Plus* **2020**, *135*, 1–12. [[CrossRef](#)]
23. Yue, C.; Khater, M.M.; Attia, R.A.; Lu, D. The plethora of explicit solutions of the fractional KS equation through liquid–gas bubbles mix under the thermodynamic conditions via Atangana–Baleanu derivative operator. *Adv. Differ. Equ.* **2020**, *2020*, 1–12. [[CrossRef](#)]
24. Khater, M.M.; Park, C.; Lu, D.; Attia, R.A. Analytical, semi-analytical, and numerical solutions for the Cahn–Allen equation. *Adv. Differ. Equ.* **2020**, *2020*, 1–12. [[CrossRef](#)]
25. Qin, H.; Khater, M.; Attia, R.A.; Lu, D. Approximate Simulations for the Non-linear Long-Short Wave Interaction System. *Front. Phys.* **2020**, *7*, 230. [[CrossRef](#)]
26. Khater, M.; Attia, R.A.; Lu, D. Computational and numerical simulations for the nonlinear fractional Kolmogorov–Petrovskii–Piskunov (FKPP) equation. *Phys. Scr.* **2020**, *95*, 055213. [[CrossRef](#)]
27. Qin, H.; Attia, R.A.; Khater, M.; Lu, D. Ample soliton waves for the crystal lattice formation of the conformable time-fractional $(N + 1)$ Sinh-Gordon equation by the modified Khater method and the Painlevé property. *J. Intell. Fuzzy Syst.* **2020**, *38*, 2745–2752. [[CrossRef](#)]
28. Khater, M.M.; Lu, D.; Attia, R.A. Dispersive long wave of nonlinear fractional Wu–Zhang system via a modified auxiliary equation method. *AIP Adv.* **2019**, *9*, 025003. [[CrossRef](#)]

29. Attia, R.A.; Lu, D.; MA Khater, M. Chaos and relativistic energy-momentum of the nonlinear time fractional Duffing equation. *Math. Comput. Appl.* **2019**, *24*, 10. [[CrossRef](#)]
30. Liang, J.F.; Wang, X. Investigation of Interaction Solutions for Modified Korteweg-de Vries Equation by Consistent Riccati Expansion Method. *Math. Probl. Eng.* **2019**, 2019. [[CrossRef](#)]
31. Liang, J.; Wang, X. Consistent Riccati expansion for finding interaction solutions of (2 + 1)-dimensional modified dispersive water-wave system. *Math. Methods Appl. Sci.* **2019**, *42*, 6131–6138. [[CrossRef](#)]
32. Zhao, Z. Bäcklund transformations, rational solutions and soliton-cnoidal wave solutions of the modified Kadomtsev–Petviashvili equation. *Appl. Math. Lett.* **2019**, *89*, 103–110. [[CrossRef](#)]
33. Thiam, L.; Liu, X.Z. Residual Symmetry Reduction and Consistent Riccati Expansion to a Nonlinear Evolution Equation. *Complexity* **2019**, 2019. [[CrossRef](#)]
34. Chen, J.; Ma, Z. Consistent Riccati expansion solvability and soliton-cnoidal wave interaction solution of a (2 + 1)-dimensional Korteweg–de Vries equation. *Appl. Math. Lett.* **2017**, *64*, 87–93. [[CrossRef](#)]
35. Bakodah, H.; Al Qarni, A.; Banaja, M.; Zhou, Q.; Moshokoa, S.P.; Biswas, A. Bright and dark Thirring optical solitons with improved Adomian decomposition method. *Optik* **2017**, *130*, 1115–1123. [[CrossRef](#)]
36. Turkyilmazoglu, M. Parametrized Adomian decomposition method with optimum convergence. *ACM Trans. Model. Comput. Simul. (TOMACS)* **2017**, *27*, 1–22. [[CrossRef](#)]
37. Turkyilmazoglu, M. Determination of the correct range of physical parameters in the approximate analytical solutions of nonlinear equations using the Adomian decomposition method. *Mediterr. J. Math.* **2016**, *13*, 4019–4037. [[CrossRef](#)]
38. Nouri, K. Study on efficiency of the Adomian decomposition method for stochastic differential equations. *Int. J. Nonlinear Anal. Appl.* **2017**, *8*, 61–68.
39. Keskin, A.Ü. Adomian decomposition method (ADM). In *Boundary Value Problems for Engineers*; Springer: Berlin/Heidelberg, Germany, 2019; pp. 311–359.
40. Satarić, M.V.; Dragić, M.S.; Sekulić, D.L. From giant ocean solitons to cellular ionic nano-solitons. *Rom. Rep. Phys.* **2011**, *63*, 624–640.
41. Gui, G.; Liu, Y.; Sun, J. A nonlocal shallow-water model arising from the full water waves with the Coriolis effect. *J. Math. Fluid Mech.* **2019**, *21*, 27. [[CrossRef](#)]
42. Slunyaev, A.; Ezersky, A.; Mouaze, D.; Chokchai, W. Standing Gravity Wave Regimes in a Shallow-Water Resonator. In *Nonlinear Waves and Pattern Dynamics*; Springer: New York, NY, USA, 2018; pp. 63–75.
43. Quirchmayr, R. A new highly nonlinear shallow water wave equation. *J. Evol. Equ.* **2016**, *16*, 539–567. [[CrossRef](#)]
44. Zahran, E.H. Exact traveling wave solutions for Nano-solitons of Ionic waves propagation along Microtubules in living cells and Nano-Ionic currents of MTs. *World J. Nano Sci. Eng.* **2015**, *5*, 78–87. [[CrossRef](#)]
45. Khater, M.M.A.; Seadawy, A.R.; Lu, D. New and more general exact and approximate solutions for the model of weakly nonlinear shallow water wave regime. *Results Phys.* **2019**, submitted.

